FEATURE EXTRACTION
OF A SINGLE DIHEDRAL REFLECTOR FROM SAR DATA

Zheng-She Liu   *Jian Li*

Department of Electrical & Computer Engineering, University of Florida, Gainesville, FL 32611-2044, USA.

ABSTRACT

As one of the key steps in the feature extraction of targets consisting of both trihedral and dihedral corner reflectors via synthetic aperture radar, this paper studies the problem of estimating the parameters of a single dihedral corner reflector. The data model of the problem and the Cramér-Rao bounds (CRBs) for the parameter estimates of the data model are presented. Two algorithms, the FFTB (fast Fourier transform based) algorithm and the NLS (non-linear least squares) algorithm, are devised to estimate the model parameters. Numerical examples show that the parameter estimates obtained with both algorithms approach the CRBs as the signal-to-noise ratio increases. The parameter estimates obtained with the NLS algorithm start to achieve the CRB at a lower SNR than those with the FFTB algorithm, while the latter algorithm is computationally more efficient.

1. INTRODUCTION

Target features are very important in many applications including automatic target classification with synthetic aperture radar (SAR). A commonly used data model in target feature extraction via SAR is the sum of several two-dimensional (2-D) sinusoids in noise. This model assumes that each target consists of several point scatterers or trihedral corner reflectors. In practice, however, many targets contain other scattering phenomena that do not behave like point scatterers [1]. For most man-made targets, the returned energy is primarily caused by trihedral as well as dihedral corner reflectors [2]. The features of a dihedral corner are completely different from those of a trihedral [3]. The former can be more important than the latter because they contain information such as the orientation of a target with respect to the radar.

A mixed data model can be used to describe both trihedral and dihedral corner reflectors. By using the relaxation-based approaches [4], one of the key issues of estimating the parameters of the mixed data model becomes estimating the parameters of a single trihedral or dihedral. The problem of estimating the parameters of trihedrals has been addressed in [4]. Hence, we concentrate on the parameter estimation of a single dihedral corner reflector in this paper.

We first introduce a data model describing the dihedral features. We then propose a computationally efficient FFTB (fast Fourier transform based) algorithm and a more sophisticated non-linear least squares (NLS) algorithm to extract the features of the data model. At low signal-to-noise ratio (SNR), the parameter estimates obtained with the FFTB algorithm are not as accurate as those with the NLS algorithm, but the former is faster than the later. The parameter estimates obtained with the FFTB algorithm can also be used as initial conditions of the NLS algorithm and can greatly speed up the convergence of the latter.

2. PROBLEM FORMULATION

It is well-known that the signal reflected by an ideal point scatterer of a radar target in a SAR system can be described as the following 2-D complex sinusoid:

$$s_p(m, \bar{m}) = \alpha_p e^{j2\pi(mf_p + \bar{m}\bar{f}_p)}, \quad \begin{array}{l} m = 0, 1, \cdots, M-1, \\ \bar{m} = 0, 1, \cdots, \bar{M}-1, \end{array}$$

$$(1)$$

where the complex amplitude α_p and the 2-D frequency pair $\{f_p, \bar{f}_p\}$, respectively, are proportional to the RCS (radar cross section) and the 2-D location (range and cross range) of the scatterer, and M and $\bar{M}$ denote the numbers of available data samples.

For a trihedral corner reflector, the RCS can be approximately considered as a constant because the angle variation of the radar beam in a SAR system is very small [3, 5]. Thus, the reflected signal of a trihedral corner reflector can be approximately described as:

$$s_t(m, \bar{m}) = \alpha_t e^{j2\pi(mf_t + \bar{m}\bar{f}_t)}, \qquad (2)$$

where α_t and $\{f_t, \bar{f}_t\}$ are proportional to the RCS and the location of the trihedral corner, respectively.

For a dihedral corner reflector, however, the RCS cannot be approximately considered to be a constant. The maximal value of the RCS is achieved when the radar beam is perpendicular to the dihedral corner. It falls off approximately as a function of $\text{sinc}(\theta) \triangleq \sin\theta/\theta$ when the angle between the radar beam and the line that is perpendicular to the dihedral corner increases [6]. The reflected signal of a dihedral corner reflector can be described as

$$s_d(m, \bar{m}) = \alpha_d \text{sinc}[\pi b(m - \tau)] e^{j2\pi(mf_d + \bar{m}\bar{f}_d)}, \qquad (3)$$

where α_d, $\{f_d, \bar{f}_d\}$, and b, respectively, are proportional to the maximal RCS, the central location, and the length of the dihedral corner, and τ denotes the peak location of the data sequence and is determined by the orientation of the

dihedral reflector. Note that this signal is a one-dimensional (1-D) rectangular pulse with width b and magnitude α_d/b in the frequency domain.

When a radar target consists of K_t trihedral and K_d dihedral corner reflectors, the data model of a realistic SAR system can be described as

$$y(m, \bar{m}) = \tilde{s}_t(m, \bar{m}) + \tilde{s}_d(m, \bar{m}) + e(m, \bar{m}), \qquad (4)$$

where

$$\tilde{s}_t(m, \bar{m}) = \sum_{k=1}^{K_t} \alpha_{t_k} e^{j2\pi \left\{ m f_{t_k} + \bar{m} \bar{f}_{t_k} \right\}} \qquad (5)$$

denotes the signal corresponding to the K_t trihedral corners,

$$\tilde{s}_d(m, \bar{m}) = \sum_{k=1}^{K_d} \alpha_{d_k} \operatorname{sinc}[\pi b_k(m - \tau_k)] e^{j2\pi \left(m f_{d_k} + \bar{m} \bar{f}_{d_k} \right)}, \quad (6)$$

denotes the signal corresponding to the K_d dihedral corners, and $e(m, \bar{m})$ denotes the 2-D unknown noise. The unknown parameters $\{\alpha_{t_k}, f_{t_k}, \bar{f}_{t_k}\}_{k=1}^{K_t}$ and $\{\alpha_{d_k}, b_k, f_{d_k}, \bar{f}_{d_k}, \tau_k\}_{k=1}^{K_d}$ are our features of interest and are to be estimated from $\{y(m, \bar{m})\}$.

The NLS estimation of the unknown parameters $\{\alpha_{t_k}, f_{t_k}, \bar{f}_{t_k}\}_{k=1}^{K_t}$ and $\{\alpha_{d_k}, b_k, f_{d_k}, \bar{f}_{d_k}, \tau_k\}_{k=1}^{K_d}$ requires a multiple dimensional search over the parameter space. It has been shown in [4] that the relaxation-based procedure can efficiently solve this kind of problems. One of the key steps in the relaxation-based procedure is to estimate the parameters of a single trihedral and dihedral reflector. since the problem of estimating the parameters of a single trihedral reflector has been addressed in [4], we only consider the problem of extracting the features of a single dihedral corner in this paper. The data model of the problem is then described as

$$y_d(m, \bar{m}) = s_d(m, \bar{m}) + e_d(m, \bar{m}), \quad m = 0, 1, \cdots, M - 1, \\ \bar{m} = 0, 1, \cdots, \bar{M} - 1, \qquad (7)$$

where $s_d(m, \bar{m})$ is defined by (3) and $\{e_d(m, \bar{m})\}$ denotes the unknown 2-D noise sequence.

3.   THE NLS ALGORITHM

Let

$$g(m, \bar{m}) = \operatorname{sinc}[\pi b(m - \tau)] e^{j2\pi(m f_d + \bar{m} \bar{f}_d)}, \\ m = 0, 1, \cdots, M - 1, \bar{m} = 0, 1, \cdots, \bar{M} - 1, \qquad (8)$$

and let $\mathbf{Y}_d$ and $\mathbf{G}$ denote $M \times \bar{M}$ matrices whose $m\bar{m}$th element are $y_d(m, \bar{m})$ and $g(m, \bar{m})$, respectively. Then the NLS estimates of $\{\alpha_d, b, f_d, \bar{f}_d, \tau\}$ are determined by the following cost function

$$C_1 \left(\alpha_d, b, f_d, \bar{f}_d, \tau \right) = \| \mathbf{Y}_d - \mathbf{G} \alpha_d \|_F^2, \qquad (9)$$

where $\| \cdot \|_F$ denotes the Frobenius norm [7]. Minimizing C_1 in (9) with respect to α_d gives

$$\hat{\alpha}_d = \frac{\operatorname{vec}^H(\mathbf{G}) \operatorname{vec}(\mathbf{Y}_d)}{\operatorname{vec}^H(\mathbf{G}) \operatorname{vec}(\mathbf{G})}, \qquad (10)$$

where $(\cdot)^H$ denotes the complex conjugate transpose and $\operatorname{vec}[\mathbf{X}]$ denotes the vector $\begin{bmatrix} \mathbf{x}_1^T & \mathbf{x}_2^T & \cdots & \mathbf{x}_K^T \end{bmatrix}^T$ with $\{\mathbf{x}_k\}_{k=1}^K$ being the columns of $\mathbf{X}$. Since

$$\operatorname{vec}^H(\mathbf{G}) \operatorname{vec}(\mathbf{G}) = \sum_{m=0}^{M-1} \sum_{\bar{m}=0}^{\bar{M}-1} \operatorname{sinc}^2[\pi b(m - \tau)] \\ = \bar{M} \sum_{m=0}^{M-1} \operatorname{sinc}^2[\pi b(m - \tau)] = \bar{M} \|\mathbf{g}\|^2, \qquad (11)$$

where

$$\mathbf{g} = \begin{bmatrix} g(0) & g(1) & \cdots & g(M - 1) \end{bmatrix}^T, \qquad (12)$$

with

$$g(m) = \operatorname{sinc}[\pi b(m - \tau)] e^{j2\pi m f_d}, \qquad (13)$$

and $(\cdot)^T$ denoting the transpose and

$$\operatorname{vec}^H(\mathbf{G}) \operatorname{vec}(\mathbf{Y}_d) = \mathbf{g}^H \mathbf{Y}_d \mathbf{a}_{\bar{M}}^*(\bar{f}_d), \qquad (14)$$

with $(\cdot)^*$ denoting the complex conjugate and

$$\mathbf{a}_{\bar{M}}(\bar{f}_d) = \begin{bmatrix} 1 & e^{j2\pi \bar{f}_d} & \cdots & e^{j2\pi(\bar{M}-1)\bar{f}_d} \end{bmatrix}^T, \qquad (15)$$

we can rewrite (10) as

$$\hat{\alpha}_d = \frac{\mathbf{g}^H \mathbf{Y}_d \mathbf{a}_{\bar{M}}^*(\bar{f}_d)}{\bar{M} \|\mathbf{g}\|^2}. \qquad (16)$$

By inserting (10) into (9), (9) can be simplified to

$$C_2 \left(b, f_d, \bar{f}_d, \tau \right) = \operatorname{vec}^H(\mathbf{Y}_d) \operatorname{vec}(\mathbf{Y}_d) \\ - \frac{\operatorname{vec}^H(\mathbf{Y}_d) \operatorname{vec}(\mathbf{G}) \operatorname{vec}^H(\mathbf{G}) \operatorname{vec}(\mathbf{Y}_d)}{\operatorname{vec}^H(\mathbf{G}) \operatorname{vec}(\mathbf{G})}, \qquad (17)$$

which is minimized by maximizing

$$\begin{aligned} C_3 \left(b, f_d, \bar{f}_d, \tau \right) &= \frac{\operatorname{vec}^H(\mathbf{Y}_d) \operatorname{vec}(\mathbf{G}) \operatorname{vec}^H(\mathbf{G}) \operatorname{vec}(\mathbf{Y}_d)}{\operatorname{vec}^H(\mathbf{G}) \operatorname{vec}(\mathbf{G})} \\ &= \frac{\left| \mathbf{g}^H \mathbf{Y}_d \mathbf{a}_{\bar{M}}^*(\bar{f}_d) \right|^2}{\bar{M} \|\mathbf{g}\|^2}. \end{aligned} \qquad (18)$$

The maximization of C_3 in (18) requires a four-dimensional search over the parameter space. There are several algorithms that can be used to solve this problem. In this paper, we use an alternating maximization procedure by alternatively updating b, τ, and $\{f_d, \bar{f}_d\}$ while fixing the remaining parameter estimates to maximize C_3. Note that for some given b and τ, $\|\mathbf{g}\|$ is a constant. Thus, the estimate of the frequency pair $\{f_d, \bar{f}_d\}$ is determined by maximizing $\left| \mathbf{g}^H \mathbf{Y}_d \mathbf{a}_{\bar{M}}^*(\bar{f}_d) \right|$, which can be efficiently calculated by using the 2-D FFT.

4.   THE FFTB ALGORITHM

The FFTB algorithm is devised since it is computationally more efficient than NLS and can be used to provide initial conditions to the NLS algorithm. Note that the signal $\{s_d(m, \bar{m})\}$ is a rectangular pulse in the frequency domain located at the frequency interval from $\{f_d - \frac{b}{2}, \bar{f}_d\}$ to $\{f_d + \frac{b}{2}, \bar{f}_d\}$. Let $\{Y_d(f, \bar{f})\}$ denote the 2-D FFT of the data sequence $\{y_d(m, \bar{m}), m = 0, 1, \cdots, M - 1, \bar{m} = 0, 1, \cdots, \bar{M} - 1\}$. For sufficiently high SNR, $|Y_d(f, \bar{f})|$ can be used to provide good estimates of b and $\{f_d, \bar{f}_d\}$. (Note that padding with zeros
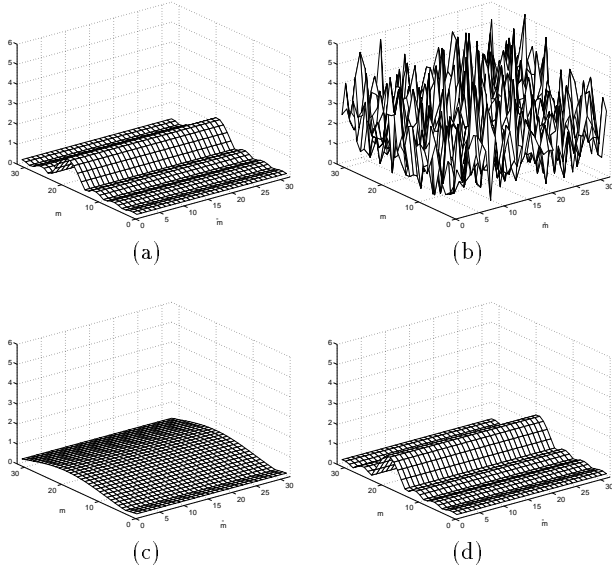
Figure 1. *Comparison of NLS and FFTB when $M = \bar{M} = 32$ and SNR= -14 dB: (a) $|s_d(m, \bar{m})|$, (b) $|y_d(m, \bar{m})|$, (c) $|\hat{s}_d(m, \bar{m})|$ estimated by FFTB, and (d) $|\hat{s}_d(m, \bar{m})|$ estimated by NLS.*

before performing the FFT is necessary to determine the estimates of b and $\{f_d, \bar{f}_d\}$ with high accuracy.) We determine their estimates with the following steps.

Step 1: Calculate the 2-D FFT $\left\{ Y_d(f, \bar{f}) \right\}$ of the data matrix $\mathbf{Y}_d$ and search the complex height $\breve{\mathbf{Y}}_d$ and the location $\{\breve{f}_d, \breve{\bar{f}}_d\}$ of the dominant peak of $\left\{ |Y_d(f, \bar{f})| \right\}$.

Step 2: Let $\{\breve{f}_{dl}, \breve{\bar{f}}_d\}$ and $\{\breve{f}_{dr}, \breve{\bar{f}}_d\}$ be the frequency pairs nearest $\{\breve{f}_d, \breve{\bar{f}}_d\}$, where $\breve{f}_{dl}$ and $\breve{f}_{dr}$ are smaller and larger than $\breve{f}_d$, respectively, such that $\left| Y_d(\breve{f}_{dl}, \breve{\bar{f}}_d) \right| < \frac{|\breve{Y}_d|}{2}$ and $\left| Y_d(\breve{f}_{dr}, \breve{\bar{f}}_d) \right| < \frac{|\breve{Y}_d|}{2}$.

Step 3: Determine the estimates $\hat{b}$, $\hat{f}_d$, and $\hat{\bar{f}}_d$, respectively, with

$$\hat{b} = \breve{f}_{dr} - \breve{f}_{dl}, \qquad (19)$$

$$\hat{f}_d = \frac{\breve{f}_{dl} + \breve{f}_{dr}}{2}, \qquad (20)$$

and

$$\hat{\bar{f}}_d = \breve{\bar{f}}_d. \qquad (21)$$

The estimate $\hat{\tau}$ of τ could be obtained by searching the dominant peak of the data sequence $\{|y_d(m, \bar{m})|\}$. To determine $\hat{\tau}$ with high accuracy, time domain interpolation of the data sequence $\{|y_d(m, \bar{m})|\}$ would be needed. Yet our FFTB algorithm determines $\hat{\tau}$ with a 1-D search method such as the golden section approach [8] by maximizing C_3 in (18) with b, f_d, and $\bar{f}_d$ in (18) replaced by their FFTB estimates. $\hat{\tau}$ obtained with this 1-D search method is usually more accurate than that obtained with the time domain interpolation since the accuracy of the latter approach is limited by the sampling interval and hence does not achieve the CRB even at high SNR. After $\hat{b}$, $\hat{f}_d$, $\hat{\bar{f}}_d$, and $\hat{\tau}$ are determined, $\hat{\alpha}_d$ is calculated with (16).
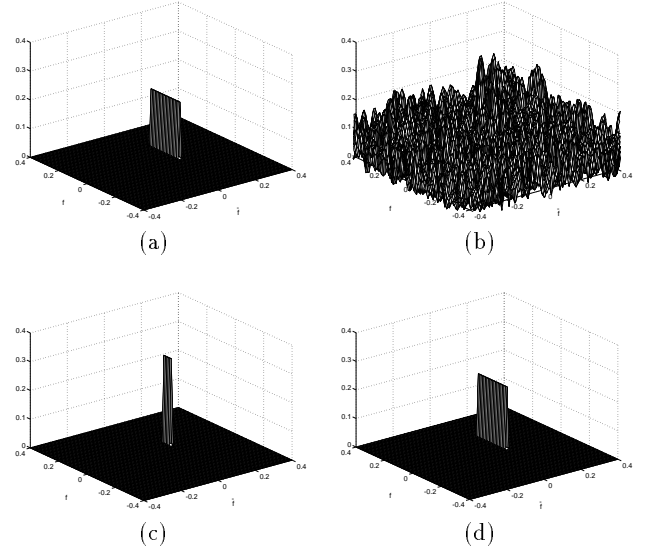

Figure 2. *Comparison of NLS and FFTB when $M = \bar{M} = 32$ and SNR= -14 dB: (a) normalized modulus of the true pulse, (b) normalized modulus of the 2-D FFT of $\{y_d(m, \bar{m})\}$, (c) normalized modulus of the pulse estimated by FFTB, and (d) normalized modulus of the pulse estimated by NLS.*

5. CRB OF THE 2-D DATA MODEL

To quantitatively compare the performances of the NLS and the FFTB algorithms, we derive the CRB for the data model (7). Let $\mathbf{Q} = \mathrm{E}\{\mathrm{vec}(\mathbf{E}_d)\mathrm{vec}^H(\mathbf{E}_d)\}$ be the 2-D noise covariance matrix, where $\mathbf{E}_d$ is an $M \times \bar{M}$ matrix whose $m\bar{m}$th element is $e_d(m, \bar{m})$. The extended Slepian-Bangs' formula for the ijth element of the Fisher information matrix has the form [9]:

$$\{\mathbf{F}\}_{ij} = \mathrm{tr}\left(\mathbf{Q}^{-1}\mathbf{Q}_i'\mathbf{Q}^{-1}\mathbf{Q}_j'\right) + 2\mathrm{Re}\left\{(\alpha_d^*\mathbf{g}^H)_i'\mathbf{Q}^{-1}(\mathbf{g}\alpha_d)_j'\right\}, \qquad (22)$$

where $\mathbf{X}_i'$ denotes the derivative of $\mathbf{X}$ with respect to the ith unknown parameter, $\mathrm{tr}(\mathbf{X})$ denotes the trace of $\mathbf{X}$, and $\mathrm{Re}(\mathbf{X})$ denotes the real part of $\mathbf{X}$. Note that $\mathbf{F}$ is block diagonal since $\mathbf{Q}$ does not depend on the parameters in $(\mathbf{g}\alpha_d)$, and $(\mathbf{g}\alpha_d)$ does not depend on the elements of $\mathbf{Q}$. Hence the CRB of the dihedral parameters can be obtained from the inverse of the second term in the right side of (22).

Let

$$\mathbf{q} = \begin{bmatrix} \mathrm{Re}(\alpha_d) & \mathrm{Im}(\alpha_d) & b & f_d & \bar{f}_d & \tau \end{bmatrix}^T. \qquad (23)$$

Then

$$\mathrm{CRB}(\mathbf{q}) = \left[2\mathrm{Re}(\mathbf{P}^H\mathbf{Q}^{-1}\mathbf{P})\right]^{-1}, \qquad (24)$$

where

$$\mathbf{P} = \begin{bmatrix} \mathrm{vec}(\mathbf{G}) & j\mathrm{vec}(\mathbf{G}) & \left(\frac{\partial \mathrm{vec}(\mathbf{G})}{\partial b}\right)\alpha_d \\ \left(\frac{\partial \mathrm{vec}(\mathbf{G})}{\partial f_d}\right)\alpha_d & \left(\frac{\partial \mathrm{vec}(\mathbf{G})}{\partial \bar{f}_d}\right)\alpha_d & \left(\frac{\partial \mathrm{vec}(\mathbf{G})}{\partial \tau}\right)\alpha_d \end{bmatrix}. \qquad (25)$$
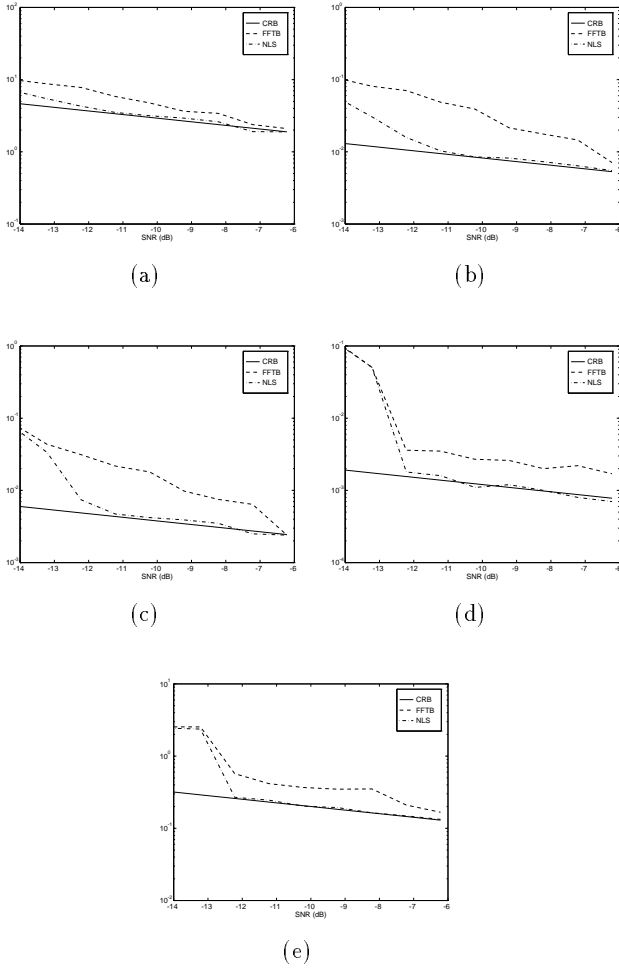
(a)

(b)

(c)

(d)

(e)

Figure 3. *Comparison of the CRBs and the RMSEs of (a) $\hat{\alpha}_d$, (b) $\hat{B}$, (c) $\hat{f}_d$, (d) $\hat{\bar{f}}_d$, and (e) $\hat{\tau}$ obtained by FFTB and NLS.*

6.   NUMERICAL EXAMPLES

We now present a numerical example comparing the performances of the NLS and FFTB algorithms with the corresponding CRBs. In this example, we choose $\alpha_d = 0.4\pi$, $b = 0.2$ Hz, $f_d = 0.1$ Hz, $\bar{f}_d = 0.1$ Hz, $\tau = 18.6$, and $M = \bar{M} = 32$. The noise sequence $\{e_d(m, \bar{m})\}$ is assumed to be a zero-mean circularly symmetric white Gaussian random process with variance σ_n^2. The SNR is defined as

$$ \text{SNR} = 10 \log_{10} \left(\frac{\sigma_s^2}{\sigma_n^2} \right) \ \text{dB}, \qquad (26) $$

where

$$ \sigma_s^2 = \frac{1}{M\bar{M}} \sum_{m=0}^{M-1} \sum_{\bar{m}=0}^{\bar{M}-1} |s_d(m, \bar{m})|^2. \qquad (27) $$

Figures 1(a), (b), (c), and (d), respectively, show the modulus of $\{s_d(m, \bar{m})\}$, the modulus of $\{y_d(m, \bar{m})\}$, the modulus of $\{\hat{s}_d(m, \bar{m})\}$ estimated by FFTB and by NLS. Figures 2(a), (b), (c), and (d), respectively, show the normalized

modulus (modulus divided by $M\bar{M}$) of the pulse, the normalized modulus of the 2-D FFT of $\{y_d(m, \bar{m})\}$, the normalized modulus of estimated pulse obtained by FFTB and by NLS, respectively, when SNR = -14 dB. We note that the NLS estimates in Figures 1(d) and 2(d) are very close to the true ones in Figures 1(a) and 2(a), respectively, while the FFTB estimates in Figures 1(c) and 2(c) are very poor.

Figure 3 shows the comparison of the root mean-squared errors (RMSEs) for the parameter estimates obtained by the two algorithms with the corresponding CRBs as a function of the SNR. The RMSEs are obtained from 100 independent Monte-Carlo trials. We note that the parameter estimates obtained with both algorithms approach the CRBs as the SNR increases. The parameter estimates obtained with NLS start to achieve the CRBs at an SNR that is between 5 dB and 8 dB lower than those obtained with FFTB. For this example, the amount of computations required by the former is only about 1.05 times as much as that by the latter.

7.   CONCLUSIONS

We have studied how to extract the features of a single dihedral corner reflector with the FFTB algorithm and the NLS algorithm. These two algorithms can be used with relaxation based approaches to extract the features of targets with multiple dihedrals and trihedrals.

REFERENCES

[1] L. C. Trintinalia and H. Ling, "Joint time-frequency ISAR using adaptive processing," to appear in *IEEE Transactions on Antennas and Propagation*, 1996.

[2] V. Larson and L. Novak, "Polarimetric subspace target detector for SAR data based on the Huynen dihedral model," *Proceedings of SPIE*, vol. 2487, pp. 235-250, Orlando, Florida, April 1995.

[3] G. T. Ruck, D. E. Barrick, W. D. Stuart, and C. K. Krichbaum, *Radar Cross Section Hand Book*, Plenum Press, New York, 1970.

[4] J. Li and P. Stoica, "Efficient mixed-spectrum estimation with applications to target feature extraction," *IEEE Transactions on Signal Processing*, vol. 44, pp. 281-295, February 1996.

[5] D. C. Munson, Jr., J. D. O'Brien, and W. K. Jenkins, "A tomographic formulation of spotlight-mode synthetic aperture radar," *Proceedings of IEEE*, vol. 71, pp. 917, 925, August, 1983.

[6] W. C. Anderson, "Consequences of nonorthogonality on the scattering properties of dihedral reflectors," *IEEE Transactions on Antennas and Propagation*, vol. 35, pp. 1154-1159, October 1987.

[7] G. W. Stewart, *Introduction to Matrix Computations*, Academic Press, Inc., New York, 1973.

[8] B. D. Bunday, *Basic Optimization Methods*, Edward Arnold Ltd, London, 1984.

[9] W. J. Bangs, *Array Processing with Generalized Beamformers*. Ph.D. Dissertation, Yale University, New Haven, CT, 1971.